

Applying Computational Analysis in Studies of Resin Transfer Moulding

Felipe Ferreira Luz^a, Sandro Campos Amico^a, Acto de Lima Cunha^b,
Enivaldo Santos Barbosa^b, Antonio Gilson Barbosa de Lima^b

^aFederal University of Rio Grande do Sul, Porto Alegre, RS, 91501-970, Brazil.

^bFederal University of Campina Grande, Department of Mechanical Engineering, Campina Grande, PB, 58429-140, Brazil.

^afelipe.luz@ufrgs.br, ^aamico@ufrgs.br, ^bactolimacunha@yahoo.com.br, ^benivaldo.sb@gmail.com,
^bgilson@dem.ufcg.edu.br

Keywords: RTM, Numeric Analysis, Permeability, Porous Fibrous Media, Composites.

Abstract. Resin Transfer Moulding (RTM) as it is most known process in the Resin Injection's family, is an extensively studied and used processing method. This process is used to manufacture advanced composite materials made of fibres embedded in a thermoset polymer matrix. Fibre reinforcement in RTM processing of polymer composites is considered as a fibrous porous medium regarding its infiltration by the polymer resin. In this sense, the present work aims the computational analysis of a fluid in a porous media for a RTM composite moulding by using the ANSYS CFX[®] commercial software. In order to validate the numerical study of the fluid flow in a known RTM system, experiments was carried out in laboratory to characterize the fluid (vegetal oil) flowing into the porous media (0/90 glass fibre woven), were pressure and fibre volume fraction have been fixed. The numerical simulation provides information about volume fraction, pressure and velocity distribution of the phases (resin and air) inside the porous media. The predicted results were compared with the experimental data and it's has shown a solid relationship between them.

Introduction

Resin transfer molding (RTM) is a manufacturing process of composite materials where a liquid thermosetting resin is injected into a closed mold containing a dry fibrous preform (porous/fibrous media), impregnating the reinforcement for subsequent resin curing. Of the various processes of composite materials advanced manufacturing, the RTM has become very important in the industrial sector [1]. However, this process is still underutilized compared to its potential, and one of the main barriers is the reproducibility of the final properties and finishing of the parts [2], besides the understanding of the resin's flow process is necessary too. A proper characterization of the preform permeability is crucial for the flow's numerical simulation and for the real manufacturing process, thus avoiding the production of defective parts [3].

The behavior of fluids in porous media has been studied for many years and numerical analysis are recognized as an effective method to predict the variables and propose the ideal processing condition [4,5]. Because of the deeply decreased computation cost, this method was widely applied even though the generated results could be inapplicable for the actual process [6]. Given the above, this work aims to study (theoretic and experimental) the process of molding composite materials by RTM and their physical parameters (permeability and porosity of the system, fluid viscosity and filling time) to obtain a better understanding of the phenomenon.

Mathematical Model

Conservation equations

The conservation equations used in this study to explain the multiphase resin/air flow in porous medium corresponds to a generalization of the Navier-Stokes equations and the Darcy's law which are commonly used for flows in porous media. Specifically, the conservation equations of mass and momentum are as follows.

$$\frac{\partial}{\partial t}(\phi\rho) + \nabla \cdot (\rho\mathbf{K} \times \vec{U}) = 0 \quad (1)$$

$$\frac{\partial (\rho\phi\vec{U})}{\partial t} + \nabla \cdot (\rho\phi(\mathbf{K}\vec{U}) \otimes \vec{U}) - \nabla \cdot (\mu_e \mathbf{K} (\nabla \vec{U} + \nabla \vec{U}^T)) = -\phi \mathbf{R} \cdot \vec{U} - \phi \nabla p \quad (2)$$

where \vec{U} corresponds to the actual velocity vector, t is time, ϕ is the porosity, ρ stands for density, and $\mathbf{K} = (K^{ij})$ is a symmetric tensor of second order called area porosity tensor; μ_e corresponds to the effective viscosity and $\mathbf{R} = (R^{ij})$ represents the flow resistance in porous medium.

In situations of high flow resistance a high pressure gradient must be assigned in order to balance the resistance. In this situation, the two terms of the right side of Eq. 2 are large and of opposite sign, and the convective and diffusive terms in the left side of the equation are insignificant. Thus, Eq. 2 is reduced to:

$$\mathbf{U} = -\mathbf{R}^{-1} \times \nabla p \quad (3)$$

Thus, at the high resistance limit, an anisotropic version of Darcy's law is obtained, with proportional permeability to the opposite of resistance tensor.

Initial and boundary conditions

The pre-form was initially considered as having pressure (P_i), temperature (T_i), and air saturation (S_{ai}) homogeneously distributed throughout the reservoir with the following values: $P_i = 1013.23$ mbar, $T_i = 300$ K and $S_{ai} = 1.0$ (consequently the resin saturation is $S_{ri} = 0.0$). The adopted boundary conditions are represented in Table 1.

Table 1 Boundary Conditions

Boundary	f_a	f_r	P (mbar)	\vec{v} (m/s)	T (K)
Inlet	0	1	Eq. (4)	-	300
Outlet	-	-	1013.25	-	-
Walls	-	-	-	0	-

where f_a and f_r are volumetric fractions of air and resin, respectively, \vec{v} is the boundary velocity vector; T is the input resin temperature in the injection, and P is the static pressure at the inlet and outlet boundary of the pre-form. The Eq. 4 was obtained by fitting to the experimental data. It is given by:

$$P_{inj}(t) = \begin{cases} P_0 + A \cdot t^{0.25} + E \cdot e\left(\frac{B \cdot t}{C + D \cdot t}\right), & \text{for } 0 \leq t \leq t_e \\ P_e, & \text{for } t \geq t_e \end{cases} \quad (4)$$

where P_0 is the atmospheric pressure. The parameters on the Eq. 4 are represented in Table 2.

Table 2 - Constant used in Eq. 4.

	Experiment	P_e (mbar)	t_e (s)	A (mbar s ^{-0.25})	B (s ⁻¹)	C	D (s ⁻¹)	E (mbar)
V_f variation	P01V20	1078.86	40	13.61	7.09	1.29	0.62	6.01x10 ⁻⁴
	P01V30	1091.02	85	20.21	6.76	1.55	0.56	1.62x10 ⁻⁴
	P01V40	1085.81	35	25.21	8691.63	1232.42	637.45	2.74x10 ⁻⁵
P_{inj} variation	P03V40	1303.15	132	29.19	7.02	9.93	0.87	1.30x10 ⁻¹
	P05V40	1494.85	168	42.05	1.42	1.39	0.14	3.68x10 ⁻²
	P07V40	1679.72	240	30.41	-72.28	-178.62	-9.67	5.29x10 ⁻¹
	P09V40	1888.35	294	45.20	-3099.14	-6960.16	-352.70	0.18
	P10V40	2008.90	325	45.87	4.54	32.35	0.75	3.99

Experimental procedure

To validate the mathematical model and numerical procedure, several experiments were conducted of a resin injection in a porous pre-form. The Newtonian fluid used as a resin in the experiments was a commercial vegetable oil (soybean oil) with density of 914 kg/m^3 . The fluid's viscosity at a temperature of 23°C (same temperature that occurred in the experiments) was 37.1 cP , measured in a Brookfield viscometer HBDV-II + C / P with the S40 spindle. For the fibrous reinforcement, was used woven 0/90 of E-glass fiber from Owens Corning (300g/m^2). In the experiments we use the RTM mold, with radial injection, which equipment schematic is shown in Fig 1.



Fig. 1 - Photo of the RTM experimental apparatus from LACOMP/UFRGS: (a) pressure vessel, (b) strengthened glass top mold, (c) steel lower mold, (d) pressure controller, (e) pressure transducers, (f) data acquisition system and (g) camera.

When using radial infiltration in RTM, the time required (t_{ff}) for the fluid, which passes through an injection port with a radius r_{inj} and injection pressure P_{inj} (gauge), fill a region of radius r_{ff} in the mold is given by Eq. 5, where ϕ ($\phi = 1 - V_f$, V_f is the fiber's volume fraction) is the porosity of the porous fibrous media. This equation is applied only until the flow reaches the front wall of the mold.

$$K = \frac{\phi\mu}{2P_{inj}t_{ff}} \left[r_{ff}^2 \ln \left(\frac{r_{ff}}{r_{inj}} \right) - \frac{1}{2} (r_{ff}^2 - r_{inj}^2) \right] \quad (5)$$

Therefore, during the infiltration, the radius of the flow front was measured at different times and, using Eq. 5, it was determined the permeability of the medium.

The resin's injection pressure in the mold was monitored during each experiment. From the pressure data collected, was made a non-linear regression using the Mathematica[®] software resulting in a pressure equation as a function of process time, as Table 2. Several experiments were performed by varying the volumetric fiber content (V_f) and injection pressure. The parameters of the experiments, the permeability data found and the mold filling time are described in Table 3.

Table 3 - Permeability and mold filling time for several experiments.

	Experiment	V_f (%)	P_{inj} (Pa)	P_{inj} (bar) pre-set	V_f (%) pre-set	$V_{f\text{real}}$ (%)	K (10^{-11} m^2)	t_{fill} (s)
V_f variation	P01V20	23.964	7420	0.1	20	24.0	136.8	130
	P01V30	30.270	7780	0.1	30	30.3	30.9	420
	P01V40	43.410	7460	0.1	40	43.4	4.4	2280
P_{inj} variation	P03V40	41.715	28570	0.3	40	41.7	3.0	860
	P05V40	41.562	48260	0.5	40	41.6	2.5	700
	P07V40	42.242	67240	0.7	40	42.2	2.2	640
	P09V40	41.726	88450	0.9	40	41.7	2.0	560
	P10V40	41.862	99800	1.0	40	41.9	3.7	380

Numerical solution

The geometry and dimensions of the injection molding are shown in Fig. 1. It's in the mold's inside which will occur the fluid injection. For the numerical analysis was created a structured mesh with 17,532 elements and 23,876 nodes using ANSYS ICEM CFD software version 12.0.1. To perform

the numerical simulations was used the ANSYS CFX 12.1 with a time step of 0.5 s. For this numerical analysis was used a Quad Core 2.66 GHz, 8 GB RAM and 1 TB physical memory (HD) computer.

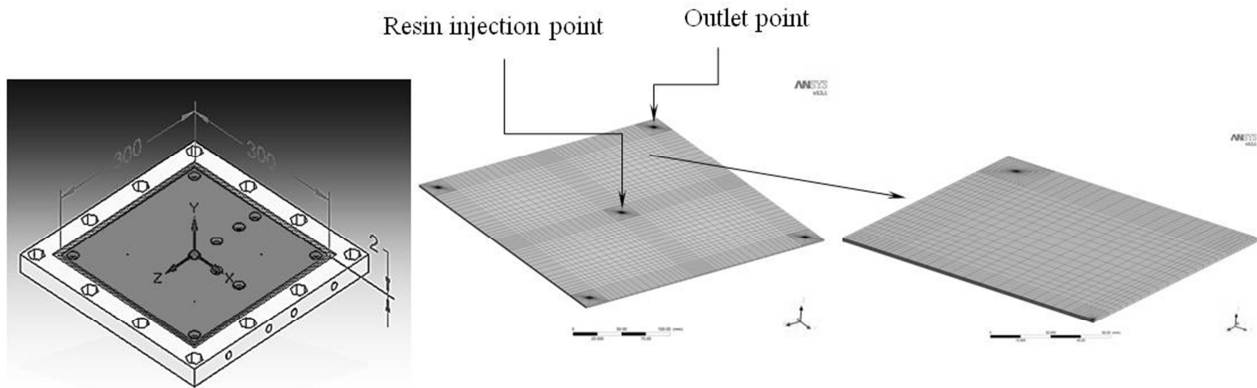


Fig. 2 - Geometry of the injection mold with the dimensions of the study area of the mold (300 x 300 x 2 mm).

Results and discussions

The volume fraction variation of the experiments and simulations were analyzed and compared. Fig. 3 shows a volume fraction comparison of the injected fluid evolution in the P09V40 case in three different times (60, 150 and 360 s). Whereas Fig 5 shows this comparison at the moment where occurs the filling of the mold (t_{fill}) from P07V40, P09V40 and P10V40 cases.

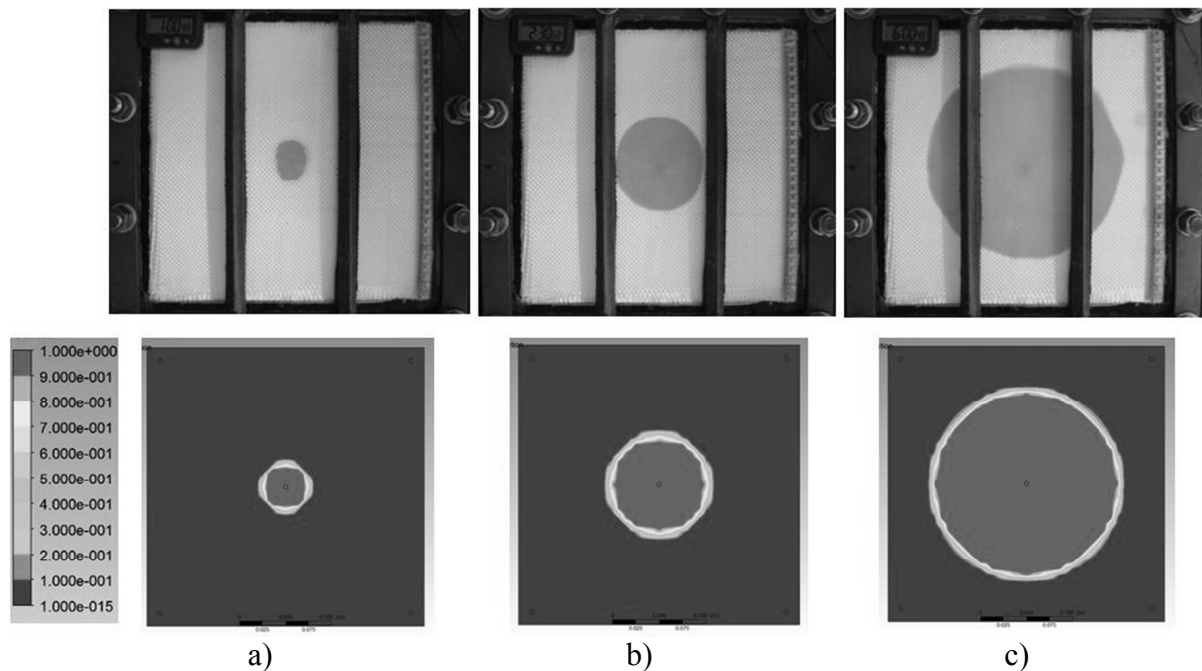


Fig. 3 - Forward flow evolution of the fluid in the case P09V40 a) 60 s, b) 150 sec) 360 s.

In Figs. 3 and 4 the darker circular areas are regions where the woven is already impregnated, and the light areas, the dry woven. It is observed that the flow fronts forms a circle, however in the simulation the permeated region forms a more defined circle than the experimental. This is because in the simulation we consider a homogeneous distribution of fibers in the woven, which it does not always happen, creating a greater concentration of fibers in certain regions, as well having a differentiated forward flow in these different regions. In all the eight cases studied, was measured the experimental and simulated radius of the flow front at time t_{fill} and the percentage error between them; these data are presented in Table 4.

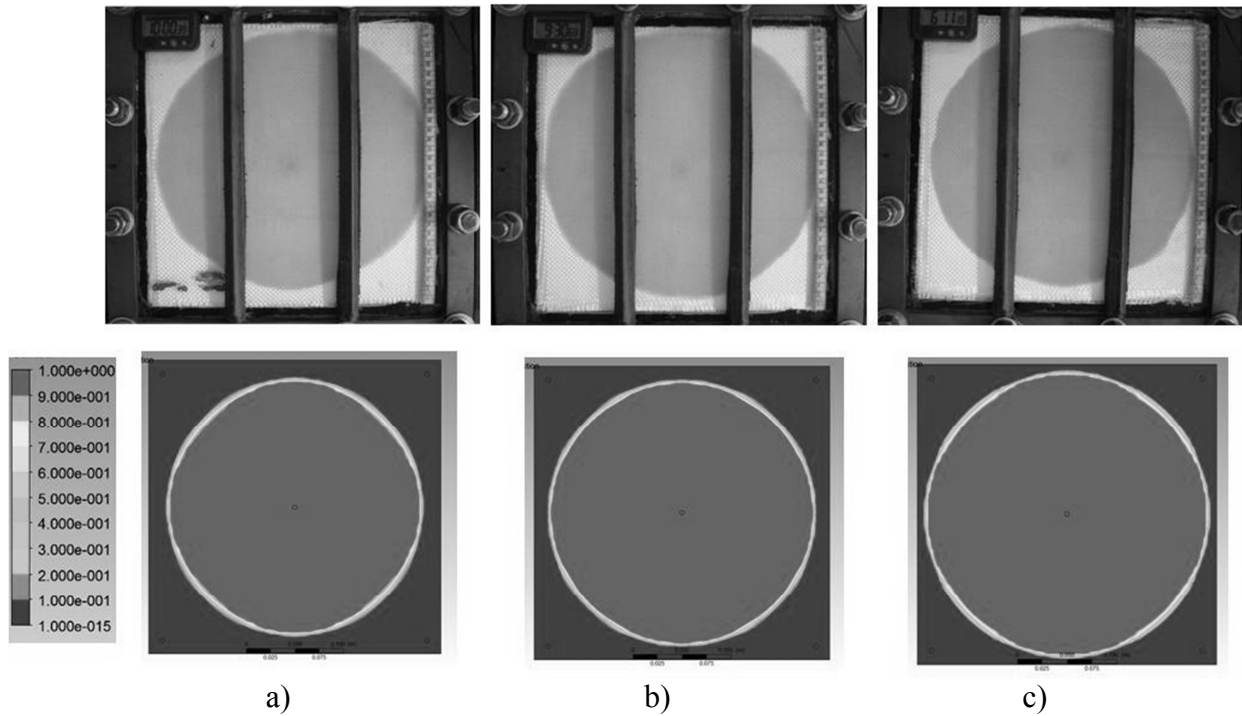


Fig. 4 - Volume fraction comparison in the t_{fill} for a) P07V40, b) P09V40 and c) P10V40 cases.

Table 3 – Comparison between the experimental and simulated flow front.

	r_{exp} (m)	r_{ansys} (m)	error (%)	t_{fill} (s)
P01V20	0.1442	0.1404	2.65%	130
P01V30	0.1351	0.1378	-1.97%	420
P01V40	0.1313	0.1231	6.21%	2280
P03V40	0.1321	0.1439	-8.96%	860
P05V40	0.1408	0.1295	8.01%	700
P07V40	0.1395	0.1301	6.77%	640
P09V40	0.1423	0.1370	3.76%	560
P10V40	0.1375	0.1402	-1.96%	380

By comparing the radius, in the Table 4, are observed errors ranging from 8.01% to -8.96%, and the negative sign indicates that the simulated radius was larger than the experiment. As there were no errors greater than 10%, the results are acceptable, showing the solid relationship between the numerical analysis of the equations of porous medium and the experimental procedure. These errors can be linked to a number of factors, particularly factors related to the experimental process, such as lack of homogeneity of the woven properties, operator error to get the measures of time, error in the measurements of the radius of forward flow and error in measures of time throughout the process.

Fig. 5 shows the pressure distribution over the mold to the t_{fill} instant for the P09V40 case. As expected, the maximum pressure is located in the fluid injection channel, and is decreasing as moved away from this point, forming a regular pressure field. This is a very representative image, as this would not be possible to observe and analyze only performing the experimental procedure.

Fig. 6a is observed the field of fluid velocity over the mold at the t_{fill} instant. The velocity is minimal in most of the mold area, with a value of 1.918×10^{-3} m/s. In the region near to the injection channel the velocity varies and has its maximum value, 1.918×10^{-2} m/s. This can be seen in detail in Fig. 6b. Since the velocities values are smaller the Darcy's law is perfectly applicable in all presented experiments.

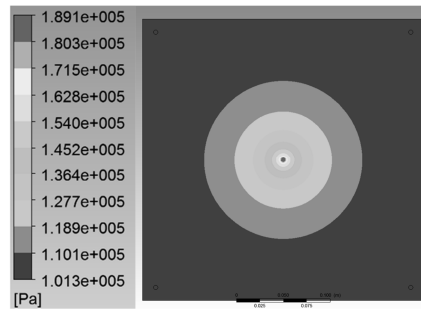


Fig. 5 - Total pressure field for the case P09V40 at $t = 560$ s (t_{fill}).

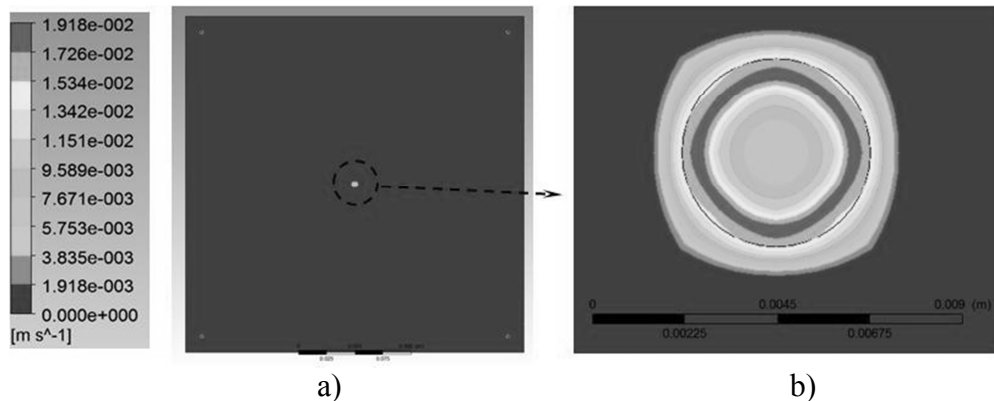


Fig. 6 - a) Velocity field of the injected fluid (resin) to the P09V40 case at $t=560$ s (t_{fill}) b) detail of the velocity field in the injection channel.

Conclusion

The porous media's equations proved to be employable in the RTM process study. The numerical analysis proved to be very reliable, with errors below 10% in the measurement of the front flow radius of the different cases. With the numerical simulation was able to have a greater understanding of the behavior of fluid flow during the RTM process, and it was possible to observe events that are not possible to be observed only by performing laboratory experiments.

Acknowledgements

The authors thanks to CNPq and CAPES for financial support, as well as to researchers referenced that with your research, helped in its improvement.

References

- [1] G. Morren, M. Bottiglieri and S. Bossuyt, H. Sol, D. Lecompte, B. Verleye, S.V. Lomov. *Composites: Part A* Vol. 40, Issue 3 (2009), p. 244.
- [2] J. Li, C. Zhang, R. Liang and B. Wang. *Composites: Part A* Vol. 36, Issue 5 (2005), p. 564.
- [3] K. Hoes, D. Dinescu, H. Sol, M. Vanheule, R. S. Parnas, Y. Luo and I. Verpoest. *Composites: Part A* Vol. 33, Issue 7 (2002), p. 959.
- [4] K. K. Han, C.W. Lee and B.P. Rice. *Composites Science and Technology*, Vol. 60, Issues 12-13 (2000), p. 2435.
- [5] A. Shojaei, S. R. Ghaffarian and S. M. H. Karimian. *Composite Structures* Vol. 65, Issues 3-4 (2004), p. 381.
- [6] F. Shin and X. Dong. *Finite Elements in Analysis and Design* Vol. 47, Issues 77 (2011), p. 764.